EPJ Web of Conferences **69**, 00008 (2014)
DOI: 10.1051/epjconf/20146900008

Elastic and inelastic scattering of neutrons on ^{238}U nucleus

R. Capote[1,a], A. Trkov[1,2], M. Sin[3], M.W. Herman[4], and E.Sh. Soukhovitskiĭ[5]

[1] *NAPC–Nuclear Data Section, International Atomic Energy Agency, PO Box 100, Vienna A–1400, Austria*
[2] *Jožef Stefan Institute, Jamova cesta 39, Ljubljana SI–1000, Slovenia*
[3] *Nuclear Physics Department, Bucharest University, Bucharest-Magurele RO–077125, Romania*
[4] *National Nuclear Data Center, Brookhaven National Laboratory, Upton, NY 11973–5000, USA*
[5] *Joint Institute for Energy and Nuclear Research, Minsk-Sosny 220109, Belarus*

Abstract. Advanced modelling of neutron induced reactions on the ^{238}U nucleus is aimed at improving our knowledge of neutron scattering. Capture and fission channels are well constrained by available experimental data and neutron standard evaluation. A focus of this contribution is on elastic and inelastic scattering cross sections. The employed nuclear reaction model includes – a new rotational-vibrational dispersive optical model potential coupling the low-lying collective bands of vibrational character observed in even-even actinides; – the Engelbrecht-Weidenmüller transformation allowing for inclusion of compound-direct interference effects; – and a multi-humped fission barrier with absorption in the secondary well described within the optical model for fission. Impact of the advanced modelling on elastic and inelastic scattering cross sections including angular distributions and emission spectra is assessed both by comparison with selected microscopic experimental data and integral criticality benchmarks including measured reaction rates (e.g. JEMIMA, FLAPTOP and BIG TEN). Benchmark calculations provided feedback to improve the reaction modelling. Improvement of existing libraries will be discussed.

Introduction

^{238}U is a major component of nuclear fuel in commercial power reactors. Therefore its nuclear data are one of the most important sources of uncertainty of neutron transport calculations in the reactor core. Recently, tight target uncertainties in the fast neutron region on the capture and inelastic scattering data for major actinides were derived from advanced reactor sensitivity studies [1]. An IAEA Technical Meeting on "Inelastic Scattering and Capture Cross-sections Data of Major Actinides in the Fast Neutron Region" was recently held at IAEA Headquarters, Vienna, Austria to review the status of nuclear data libraries for these cross sections, and to evaluate what advances in nuclear modelling and measurement technique may improve our knowledge of these cross sections [2]. It was constated that the present status of evaluated data files for inelastic scattering is not satisfactory. Significant differences in the evaluated ^{238}U inelastic cross section are observed in the latest evaluations [3–7] as shown in Fig.1(a). Those differences lead to large cross-section uncertainties for the ^{238}U(n,n') reaction. Discrepancies are especially large in the energy region from a few hundred keV up to 2 MeV,

[a] e-mail: r.capotenoy@iaea.org

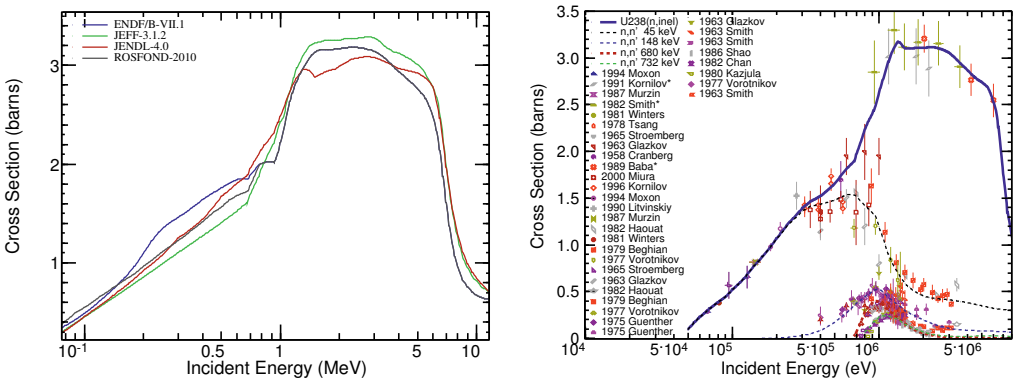

(a) Evaluated total inelastic ^{238}U(n,n') cross sections

(b) Total and partial inelastic ^{238}U(n,n') cross sections

Figure 1. (a) Discrepancies in the evaluated total ^{238}U(n,n') cross section in different nuclear data libraries [4–7]. (b) EMPIRE calculated total and partial inelastic ^{238}U(n,n') cross sections on the 45 and 148 keV levels (ground-state band), and 680 and 732 keV levels (octupole vibrational band). The experimental data were taken from the EXFOR database [8].

which corresponds to the maximum of the neutron spectrum in fast systems. While neutron scattering on the ^{238}U ground-state rotational band below 600 keV is well described by a rigid rotor model, above 600 keV several vibrational bands are observed (e.g. see estimated scattering cross sections on 1^- (680 keV) and 3^- (732 keV) states of the octupole vibrational band in Fig.1(b) compared with available experimental data from the EXFOR database [8]). Those vibrational bands need to be considered in the coupled-channel description as initially suggested by the University of Lowell group [9–11], and later used in evaluations by Kawano *et al* [12], Maslov *et al* [13, 14] and López Jimenez *et al* [15].

Participants at the above-mentioned IAEA meeting [2] recognized that fast neutron induced reactions on ^{238}U can be an ideal target to perform a compound-nucleus cross-section inter-comparison, as both fission and capture cross sections are derived in the neutron standard fit [16]). A first attempt to improve inelastic scattering cross sections was undertaken in our recently published paper [17]. The goal of the current paper is a detailed discussion of the modelling of elastic and inelastic scattering and a comprehensive comparison with available microscopic cross sections including excitation functions, angular distributions, emission spectra and double-differential measurements. Finally, an updated ^{238}U evaluated file in the fast neutron region will be validated vs integral criticality benchmarks from the ICBESP Handbook [18] aiming at reducing uncertainties in input model parameters.

1 Nuclear reaction modelling

Given the limited accuracy and availability of experimental elastic and especially inelastic scattering data on ^{238}U, nuclear reaction modelling plays a central role in the evaluation of elastic and inelastic scattering cross sections. Calculations undertaken for this contribution are based on the nuclear models implemented in the current version of the EMPIRE-3 code [19, 20] (EMPIRE 3.2.2 Malta). The nuclear reaction models include the generalized (coupled-channel) optical model, statistical equilibrium and preequilibrium models, and fission models that will be described below. Starting values for the nuclear model parameters were taken from the RIPL recommendations [21]. The generalized optical model is a fundamental theoretical tool that provides the basis of nuclear reaction modelling in the fast neutron region. The availability of suitable optical-model parameterizations serves as the

backbone of nuclear data evaluation. Using the optical model, one calculates total, elastic and reaction cross sections, but also the transmission coefficients needed in the statistical and pre-equilibrium model calculations. Thus, a unique set of optical model potential (OMP) parameters that can reproduce well the nucleon scattering data over a wide energy range is essential to make reliable nuclear data predictions.

Considerable effort has been made worldwide to derive optical model potentials (OMPs) that describe all scattering data available for nucleon-induced reactions on major actinides. Special emphasis was made to derive coupled-channel optical model potentials using dispersion relations (see Refs. [21, 22] and references therein). Dispersive integrals are calculated analytically following ref. [23]. A new rotational-vibrational dispersive optical model potential has been derived, and added to the RIPL library with the catalogue number RIPL 2412 [24, 25]. New band couplings are derived from the soft-rotor description [26, 27] of the low-lying levels of the actinides, but consistent with the rigid-rotor behaviour at low excitation energies as described in Refs. [24, 25]. Vibrational bands are described by assuming small dynamical departures (axial and non-axial quadrupole and octupole) from a larger static axial equilibrium quadrupole deformation [24, 25]. An essential innovative feature of the new potential is the coupling of 15 collective levels representing almost all excited levels below 1 MeV, including the ground state, octupole, beta, gamma, and non-axial collective bands. This is particularly important because neutron scattering on these low-lying levels plays a significant role in the energy region from 0.5 to 2 MeV of maximum interest for fast reactor systems, where major discrepancies between existing evaluations were identified. The new potential preserves the good quality of description achieved in previous actinide dispersive potentials (e.g. RIPL 2408 [21, 28])), and describes all scattering data above the resonance region up to a nucleon incident energy of 150 MeV with an energy-independent geometry and isospin dependent potential depths. Calculated total cross sections using this potential are compared with selected experimental data in Fig. 2(a); an excellent description is achieved. The same OMP is used to calculate direct contributions to uncoupled levels using the DWBA method with empirical dynamical deformations following the RIPL tabulation [21]. For the outgoing proton channel, the same potential was used as for the neutron channel, as the derived potential is valid for neutron and proton induced reactions (in RIPL, the neutron and proton potentials are stored separately. The corresponding proton OMP is RIPL 5412). For the neutrons and protons emitted by other residual nuclei and for the other emitted particles we used EMPIRE default OMPs.

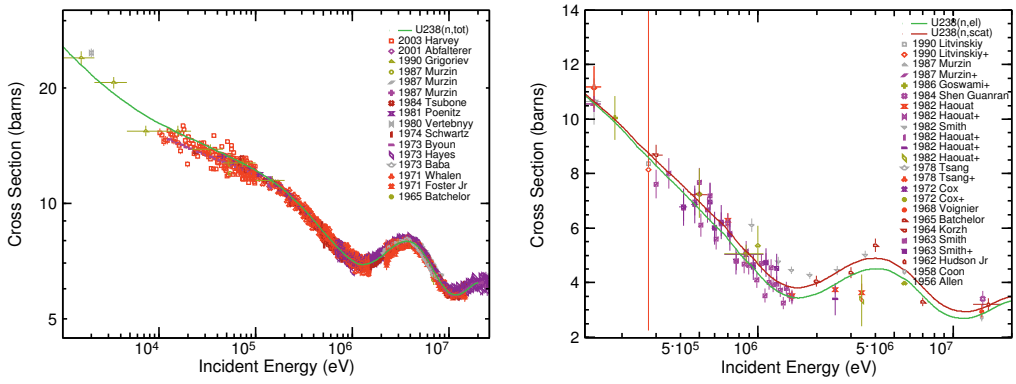

(a) ^{238}U(n,tot) cross sections

(b) ^{238}U(n,el) and ^{238}U(n,scat) cross sections

Figure 2. EMPIRE calculated total cross section (RIPL 2412 [24, 25]) (a) and elastic and scattering cross sections (RIPL 2412 [24, 25]) (b). The experimental data were taken from the EXFOR database [8].

Preequilibrium emission was considered in terms of a classical one-component exciton model (PCROSS), while the Iwamoto-Harada formalism is used for α-particle preequilibrium emission. In the case of neutrons, an important direct contribution to the continuum was calculated by the DWBA and incoherently added to the PCROSS calculated preequilibrium emission. This contribution was obtained by introducing quasi-discrete levels embedded in the continuum. Such an empirical description was compared to the quantum-mechanical description based on multi-step direct and multi-step compound MSD & MSC preequilibrium emission as implemented in EMPIRE. We preferred the former option because, in our opinion, it provides a better description of the multiple-neutron cross sections for the studied case.

The Hauser-Feshbach [29] and Hofmann-Richert-Tepel-Weidenmüller [30] versions of the statistical model were used for the compound nucleus cross section calculations. The correlation between incident and exit channels in the compound calculations (width fluctuation correction) is considered within the HRTW model up to 3 MeV incident neutron energy. Both the HF and HRTW approaches account for multiple-particle emission, the optical model for fission [31, 32] and the full gamma-cascade. A modified Lorenzian radiative-strength function (MLO) recommended by Plujko [21] was adopted for our calculations. Level densities were described by the EMPIRE-specific formalism (EGSM) in which the superfluid model was used below the critical excitation energy and the Fermi gas model above [19, 21].

1.1 Cross section calculations

Adequate validation of the results of modeling is critically dependent on the raw experimental data retrieved from the EXFOR database [8], as well as on corrections to the data due to changes in monitor reactions and reference data [33].

Calculated shape elastic cross sections using the RIPL 2412 OMP (lower green line) are compared in Fig.2(b) with the available experimental data. Unfortunately, the experimental elastic cross section data are quite scattered, which underlines the need to rely on theoretical modelling. The description of elastic data below 2 MeV is good considering the scattering of the data. Above 2 MeV, there are two groups of data, one lying higher than the second group. Available datasets highlight the fact that all measurements of the ^{238}U elastic cross section above 3.4 MeV are actually quasi-elastic measurements, as the first three excited states in ^{238}U (at 45, 148 and 307 keV) cannot be resolved from the elastic peak at those energies due to experimental limitations. Thus, all elastic data above 3.4 MeV should be considered as "quasi-elastic", and should be increased accordingly by adding cross sections from the unresolved inelastic states as shown in Fig.2(b) (upper red line). The fast energy range is of particular interest in many nuclear applications. We have identified that the calculated inelastic scattering cross sections depend on the compound nucleus decay (especially on the level density of the target nucleus defining the compound contribution) and on the optical model potential that defines the direct contribution. An interesting physical effect is demonstrated in Fig.3. As discussed by Moldauer [34], interference between two channels (e.g. neutron scattering on the ground state and first inelastic level) causes an enhancement of the fluctuating compound-nucleus (CN) cross sections in the presence of direct reactions. The strongest interference effect is expected when only two channels are open, as is precisely the case for neutron incident energies below 300 keV, where the contribution to the total inelastic cross section of scattering to the second excited level at 148 keV is very small, as seen in Fig.3. CN calculations that consider interference effects were carried out by using the Engelbrecht-Weidenmüller transformation [35] as implemented within the ECIS code [36]. The interference effect results in a net increase of the CN inelastic scattering cross section to the first excited level at 45 keV compensated by a reduction in the elastic channel (due to the reduction in the CN elastic cross section) as shown in Fig.3. This effect goes in the opposite direction to the width

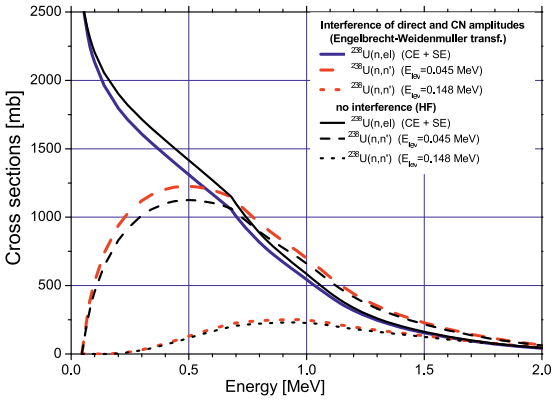

Figure 3. Effect of the Engelbrecht-Weidenmüller transformation on the ^{238}U elastic and inelastic scattering to the first two excited levels (45 and 148 keV) of the ground state band (gsb).

fluctuation correction (that increases the compound elastic at the expense of the remaining reaction channels). A comparison of the calculated total inelastic cross section with experimental data was shown in Fig.1(b). The interference effect is the main culprit in the observed increase of the calculated inelastic cross sections compared with the JEFF-3.1 [4] and JENDL-4 [5] evaluations below 500 keV. However, our calculations are still lower than the ENDF/B-VII.1 evaluation [6] in the same energy region. The current calculations produce the highest inelastic cross sections from 700 keV up to approximately 1 MeV, as a direct result of the strong coupling between all low-lying collective levels extending up to an excitation energy of 1 MeV (see Fig. 1(b)).

Calculated inelastic scattering cross sections to the first three levels of the ground-state rotational band are shown in Fig.4(a), and to selected vibrational-rotational levels in Fig.4(b,c,d). A smaller Moldauer enhancement is also obtained for inelastic scattering on other excited levels (e.g. on the octupole band levels in Fig.4(b,c)). The agreement of the calculated cross sections with the experimental data is very reasonable considering inconsistencies between the measured datasets.

Fig.5(a) presents the EMPIRE capture cross section compared to experimental data from EXFOR. The capture cross section is the dominant reaction cross section below the inelastic threshold of 45 keV. However, above the threshold the inelastic cross section becomes dominant up to 4-5 MeV neutron incident energy. The radiative capture cross section was computed using a modified Lorentzian model (MLO1) E1-strength function, with GDR parameters taken from RIPL-3 [21] and normalization to the experimental strength function around 1 keV. The differences between the calculated capture cross section and the corresponding standard cross sections [16] were very minor below 5 MeV and appeared around the inelastic threshold and in the energy region around 0.8 MeV. The discrepancy becomes significant in the energy range 5-10 MeV dominated by photon preequilibrium emission where our calculations underestimate the experimental data fitted by the standard group [16]. To make the present evaluation standard compatible, the calculations have been slightly tuned to follow the standard cross section below 1 MeV. We assumed that the absolute value of the capture cross section in the energy range 5-10 MeV is very small, and therefore not relevant for applications (and benchmarking).

The ^{238}U(n,f) cross section is a standard above 2 MeV incident energy [16]. However an extended fit was carried out down to 0.5 MeV. Unfortunately, the energy mesh used in that fit was too coarse; important experimental structures were missed (e.g. sub-threshold fission resonances at 0.9 and 1.2 MeV). Therefore, in the energy range from 0.5 up to 1.3 MeV we replaced the ENDF-B/VII.1 cross section (=STD) by the older ENDF/B-VI.8 evaluation that reproduces the observed resonance structure correctly. The fission cross section is negligible below 1 MeV, and is one fifth of the inelastic

cross section in the fission "plateau" from 2 to 5 MeV. However, the opening of the second fission chance around 6 MeV makes fission larger than the inelastic cross section and of the same order as the multiple neutron emission as shown in Fig.5(b).

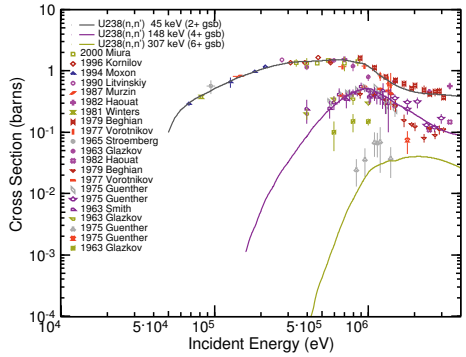

(a) ^{238}U(n,n') to the $2^+, 4^+, 6^+$ gsb levels

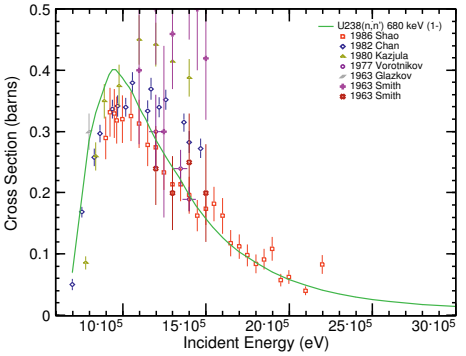

(b) ^{238}U(n,n') to the 680 keV level

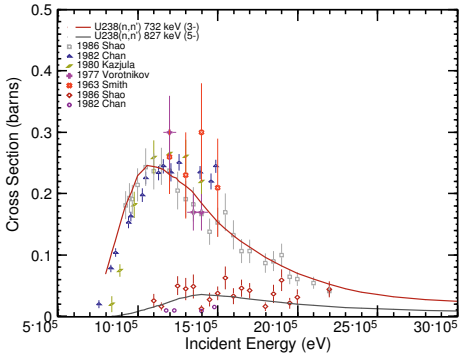

(c) ^{238}U(n,n') to the 732 and 826 keV levels

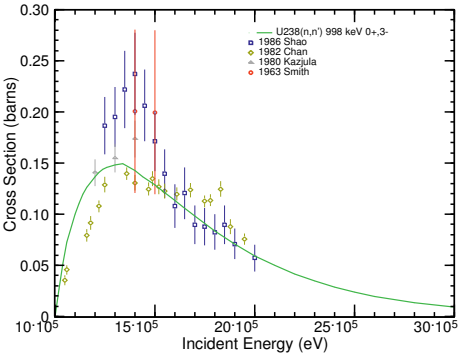

(d) ^{238}U(n,n') to the 998 keV level

Figure 4. EMPIRE calculated neutron inelastic scattering cross sections to the ^{238}U excited levels at 45, 148, and 307 keV (gsb) (a), to the excited level at 680 keV (b), to the excited levels at 732 and 827 keV (c), and to the excited level at 998 keV (d). The experimental data were taken from the EXFOR database [8].

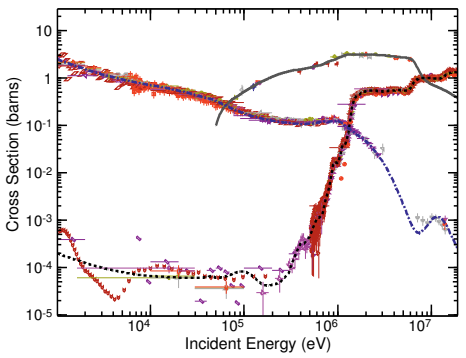

(a) ^{238}U(n,n'), ^{238}U(n,g), and ^{238}U(n,f)

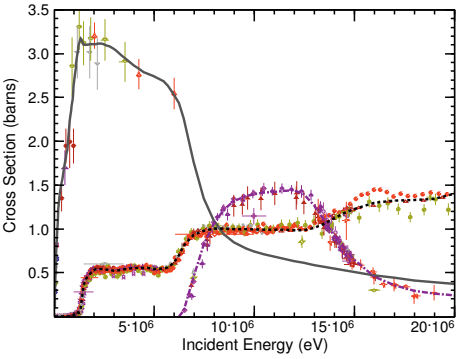

(b) ^{238}U(n,n'), ^{238}U(n,f), and ^{238}U(n,2n)

Figure 5. EMPIRE calculated ^{238}U neutron capture (dot-dashed), inelastic (solid) and fission cross sections (dashed) (a); EMPIRE calculated ^{238}U neutron inelastic (solid), fission (dashed), and (n,2n) cross sections (dot-dashed) (b). The experimental data were taken from the EXFOR database [8].

EMPIRE fission calculations were performed within the optical model for fission as implemented in the EMPIRE code [19, 31, 32] with initial parameters taken from RIPL [21] and from EMPIRE systematics. The fission mechanisms associated to the different degrees of damping of the vibrational states within the minima of the fission path (fission wells) are treated with the optical model for fission, allowing for the reproduction of the resonant structure of the fission cross section in the sub-threshold region. These default parameters have been adjusted to describe selected experimental data and to agree (within their stated uncertainties) with ENDF/B-VI.8 in the sub-threshold fission region and with the STD cross section [16] (=ENDF-VII/B-VII.1) above 2 MeV. The resulting fission cross section is also shown in Fig.5(a,b). It should be noted that the correct description of the calculated fission and capture cross section is an essential condition to predict correctly the elastic and inelastic scattering cross sections.

The calculated ^{238}U(n,2n) cross section is compared to EXFOR data in Fig.5(b). A very good description of the experimental (n,2n) cross sections is achieved, but a 5% reduction of the calculated reaction cross section was needed for a simultaneous description of the fission standard cross section and the (n,2n) one. Further investigation is warranted. Together with the fission competition, the inelastic cross section as a precursor reaction has a big impact on calculated multiple neutron emission.

1.2 Angular distribution of scattered neutrons on ^{238}U

Differential data such as angle-dependent cross sections, particle-emission spectra and double-differential cross sections defining angle-dependent particle-emission spectra are complex and usually much more difficult to measure accurately. As a rule, evaluations depend significantly on nuclear model calculations, but the choice of models and model parameters is crucial.

Assessments of the models can be made in cases where consistent experimental data are available. The average cosine of scattering $\overline{\mu}$ is a commonly employed measure of the anisotropy of elastic scattering. Experimental data derived from measured angular distributions of resolved elastic scattering for energies lower than 3.4 MeV are in excellent agreement with the smooth curve predicted by the nuclear model calculation in Fig.6(a). Such agreement demonstrates the good quality of the optical model potential employed. Unfortunately, as a more integral characteristic, the average cosine of scattering $\overline{\mu}$, is not sensitive to the fine detail observed in differential angular distributions.

Fig.6(b–f) present calculated elastic angular distributions for incident neutron energies of 55 keV up to 3.4 MeV compared to the corresponding available experimental data. An excellent agreement is shown for incident energies up to 800 keV (Fig.6(b,c,d)). The agreement indicates both the quality of the optical model potential and the right proportion between the direct and compound nucleus mechanisms. An excellent description at backward angles is also achieved due to a proper consideration of CN elastic anisotropy that is dominant in this angular region (the shape elastic mechanism results in forward scattered neutrons). The superb description of neutron backward scattering turns out to be highly important in integral benchmarks with natural or depleted uranium used as a reflector due to the relative enhancement of the backward scattering contribution. Unfortunately, this differential effect is not seen in the comparison of the average cosine of scattering $\overline{\mu}$ in Fig.6(a).

For incident neutron energies above 800 keV up to 1.25 MeV (Figs.6(d,e)) the agreement between calculations and experimental data slightly deteriorates. The explanation of this effect has not been precisely determined; obviously the experimental resolution worsens at higher energies, perhaps some contamination of the elastic angular distribution from inelastic scattering channels also took place. New measurements of elastic angular distribution around 1 MeV incident neutron energy are needed to resolve the mentioned discrepancy. At 1.5 MeV up to 3.4 MeV the agreement is almost perfect again as seen in Fig.6(f).

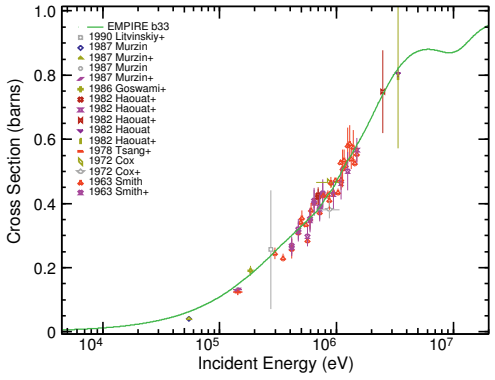

(a) ^{238}U(n,el) μ-bar

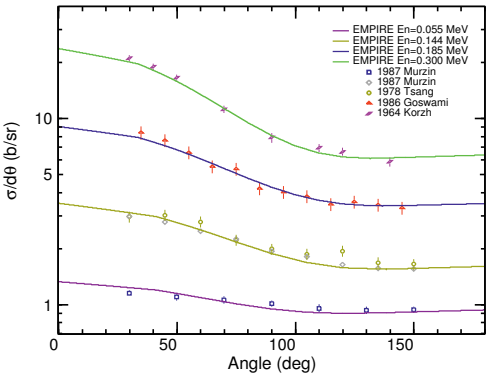

(b) ^{238}U(n,el) angular distribution

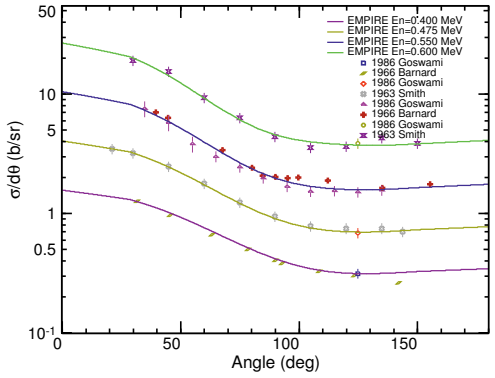

(c) ^{238}U(n,el) angular distribution

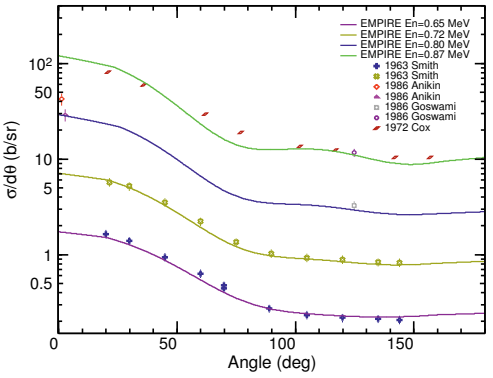

(d) ^{238}U(n,el) angular distribution

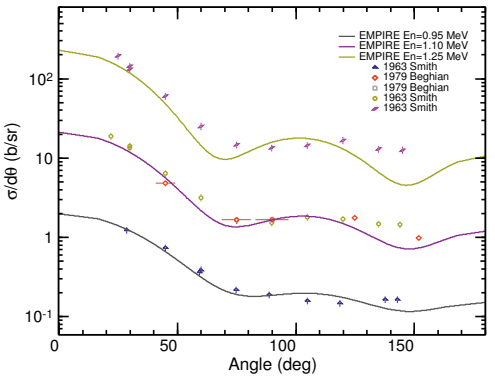

(e) ^{238}U(n,el) angular distribution

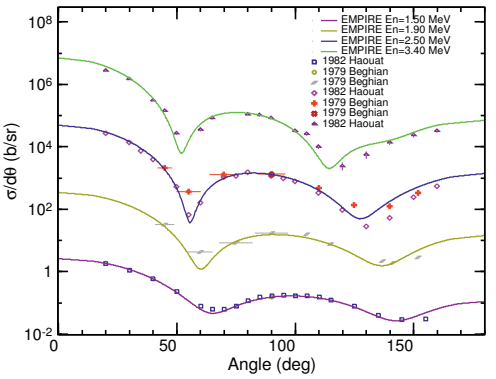

(f) ^{238}U(n,el) angular distribution

Figure 6. Average cosine of ^{238}U neutron elastic scattering (a), and ^{238}U elastic scattering angular distributions at incident neutron energies of 55–300 keV (b), 400–600 keV (c), 650–870 keV (d), 950–1250 keV (e), and 1500–3400 keV (f). The experimental data were taken from the EXFOR database [8].

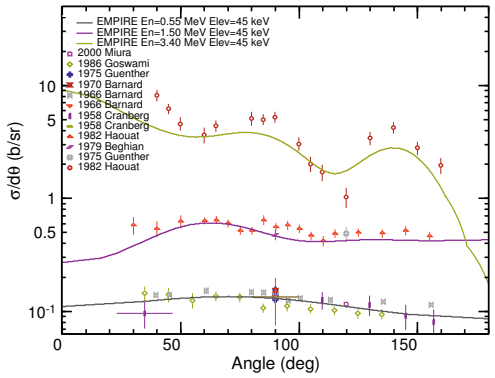

(a) ^{238}U(n,n') angular distribution, 2^+, E_{lev} = 45 keV

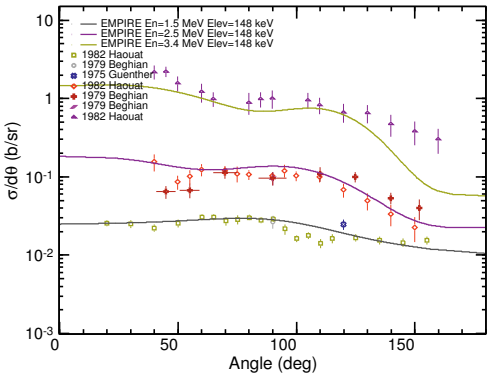

(b) ^{238}U(n,n') angular distribution, 4^+, E_{lev} = 148 keV

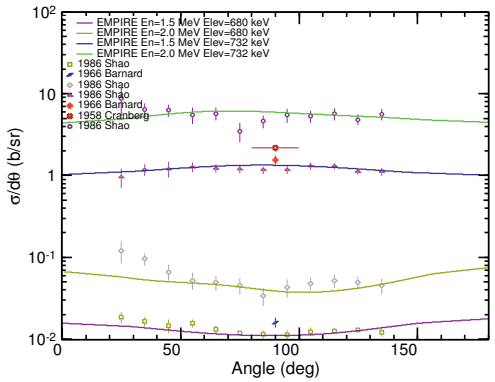

(c) ^{238}U(n,n') angular distribution, 1^-, E_{lev} = 680 keV

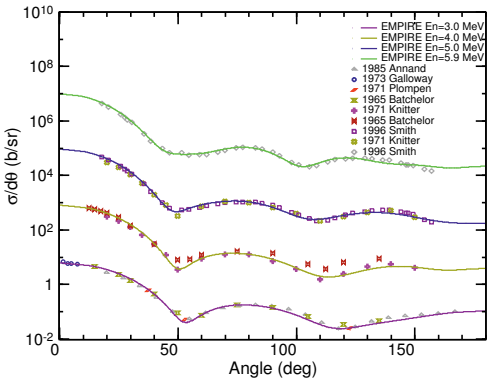

(d) ^{238}U(n,scat) angular distribution

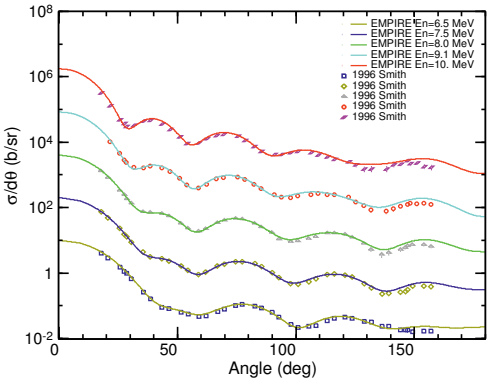

(e) ^{238}U(n,scat) angular distribution

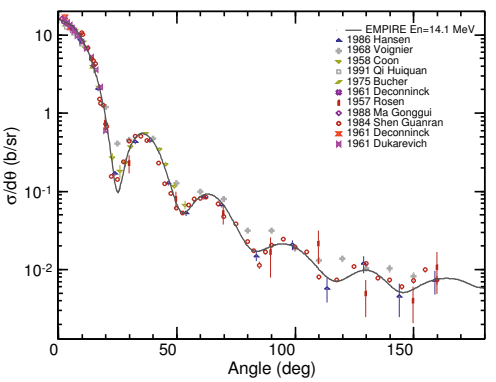

(f) ^{238}U(n,scat) angular distribution

Figure 7. EMPIRE calculated angular distributions on selected excited levels (a,b,c), and angular distributions of scattered neutrons (d,e,f) at different incident neutron energies. The experimental data were taken from the EXFOR database [8].

Figs.7(a,b,c) present EMPIRE calculated inelastic angular distributions on excited levels at 45, 148 and 680 keV (excitation energy) for incident neutron energies up to 3.4 MeV. The agreement is acceptable if we consider that the inelastic/elastic ratio implies a large background in these measurements coming from the elastically scattered neutrons. Inelastic angular ditributions depend strongly on incident neutron energy; the CN anisotropy contribution is comparatively less important than for the elastic scattering.

Figs.7(d,e,f) present EMPIRE calculated angular distributions of scattered neutrons for incident neutron energies from 3 up to 14–15 MeV. In this energy range the compound contribution is negligible, therefore all distributions are dominated by the direct reaction effects. As previously discussed all measurements were considered quasi-elastic measurements and the calculations include the contribution of the first three inelastic levels at 45,148 and 306 keV added to the elastic scattering. Typically, inelastic scattering contribution is more important in the difraction minima of the elastic scattering, and at backward angles. The observed agreement is excellent for all energies and angular ranges showing again the high quality of the description of data achieved by the dispersive coupled-channel optical model with multiple band coupling.

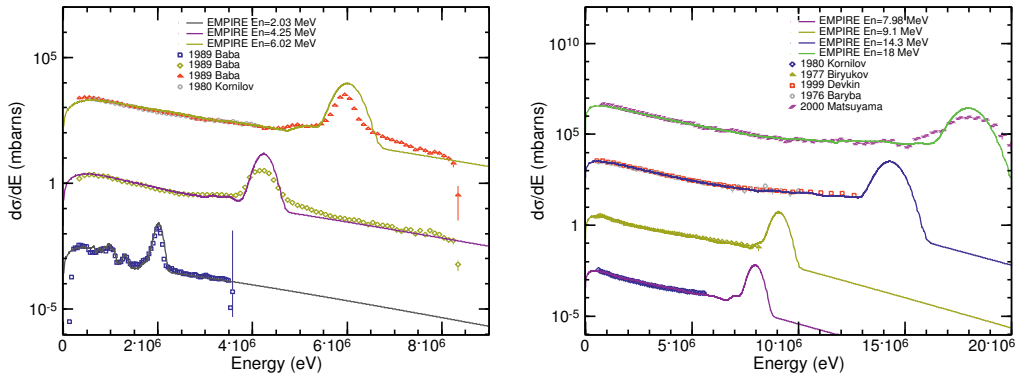

(a) Neutron emission spectra at 2.03, 4.25 and 6.1 MeV (b) Neutron emission spectra at 7.98, 9.1, 14.3 and 18 MeV

Figure 8. EMPIRE calculated neutron emission spectra at different incident neutron energies. The experimental data were taken from the EXFOR database [8].

1.3 Emission spectra of scattered neutrons on ^{238}U

The neutron emission spectra as a function of outgoing neutron energy provide very useful information about level densities and about the relative contributions of direct, pre-equilibrium and compound nucleus reaction mechanisms. Calculated neutron emission spectra are plotted in Fig.8(a,b) for incident neutron energies of 2.03 up to 18 MeV. All spectra include also the fission neutron contribution that is clearly seen at outgoing neutron energies higher than the elastic peak as a flat background. It should be noted that the description of the elastic peak is not very good. This is due to the limited number of measured angles that lead to an incomplete integration as discussed in the experimental works. At the lowest energy of 2.03 MeV we can see the importance of considering the excitation of vibrational bands, as this is the dominant contribution below the elastic scattering peak. The agreement with data in the continuum energy region below the elastic peak is very good at all energies, showing the consistency of the theoretical description of preequilibrium effects and direct scattering into the continuum.

The double-differential neutron emission spectra as a function of outgoing neutron energy provide the toughest challenge for models of neutron scattering into the continuum and the relative contributions of direct, pre-equilibrium and compound nucleus reaction mechanisms. Calculated double-differential neutron spectra are plotted in Fig.9(a–f) for incident neutron energies of 2.03 up to 18 MeV and typical outgoing angles of 30, 90, and 150 degrees. As was the case for the emission spectra, all distributions include also the fission neutron contribution that is clearly seen at outgoing neutron energies higher than the elastic peak as a flat background.

1.4 Double-differential cross sections of scattered neutrons on ^{238}U

Theoretically we expect forward scattering to be dominated by the preequilibrium and direct reaction mechanisms. There is a systematic underestimation of neutrons scattered at forward angles for energies higher than 6 MeV in the preequilibrium region as seen in Fig.9(d,e,f). The observed underestimation could be related to deficiencies in the employed preequilibrium model (exciton model). Fortunately, these energies are not very important for reactor applications, and uranium is not an important material in fusion applications. Very good agreement can be seen for the lowest incident neutron energy of 2.03 MeV in Fig.9(a), where the neutron scattering is dominated by direct reactions. The observed discontinuity around 700 keV of neutron outgoing energy is related to the maximum discrete level energy of 1.3 MeV in the target nucleus (defined by the maximum number of discrete levels of 40 allowed in the ENDF-6 format). Overall we consider the quality of emission spectra to be much improved in the current calculations. However, future quantum-mechanical model calculations may be able to improve the description of available data especially at energies higher than 6 MeV.

2 ENDF file assembly

The present results do not represent a proper evaluation that consistently includes experimental data as discussed in ref. [33], but a theory-based evaluation consistent with fission and capture standard cross sections [16] that describes differential and integral experimental data better than existing evaluations. Our results have been obtained going through the following steps:

- Model calculations have been performed in the energy range 1 keV-30 MeV with the EMPIRE 3.1 (Rivoli) code which became EMPIRE 3.2 (Malta) in January 2014.
- The initial values of the model parameters taken from RIPL have been tuned and the reaction models have been improved to fit all available differential data.
- An ENDF-6 file was assembled using our results for the fast energy range merged with resonance data and fission neutrons from the ENDF/B-VII.1 file [6]. For all benchmarking studies presented here, the calculated fission and capture cross sections were also replaced by the corresponding cross-section data (MF=3, MT=18, 102) from the ENDF/B-VII.1 file [6]. ENDF/B-VII.1 adopted the IAEA-WPEC-CSEWG neutron standards [16]. The calculated fission and capture cross sections are very close to the standards, but the replacement reduces the variability of the results in highly-sensitive criticality benchmark calculations and allows one to focus on the impact of elastic and inelastic scattering.
- Based on this ENDF-6 file, integral and quasi-differential quantities have been generated and compared with the corresponding experimental data. A comparison with the quasi-differential measurements by Danon et al. undertaken at RPI [37] was very important to achieve our goals, but was already discussed in our ND2013 contribution [17]. The results of these comparisons were used as a guide for further adjustment of input parameters. It is important to underline that the adjustments

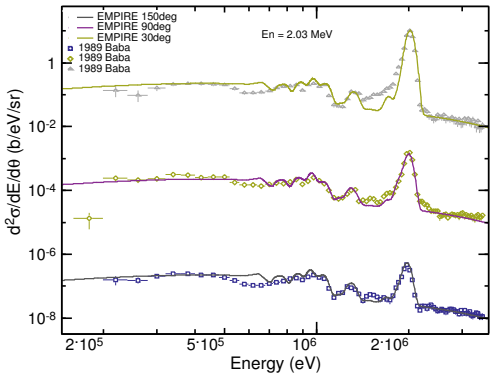

(a) Double-differential neutron emission spectra

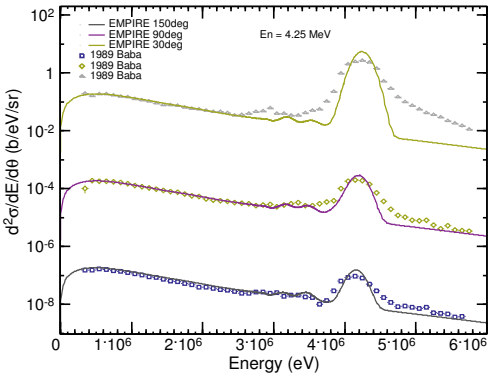

(b) Double-differential neutron emission spectra

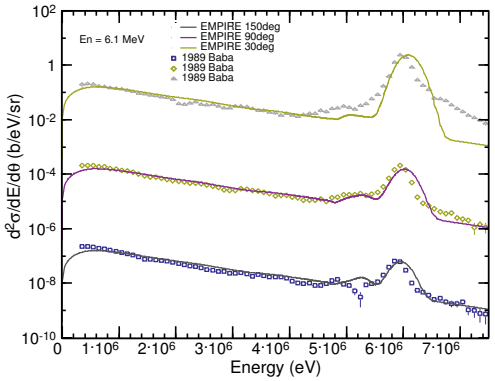

(c) Double-differential neutron emission spectra

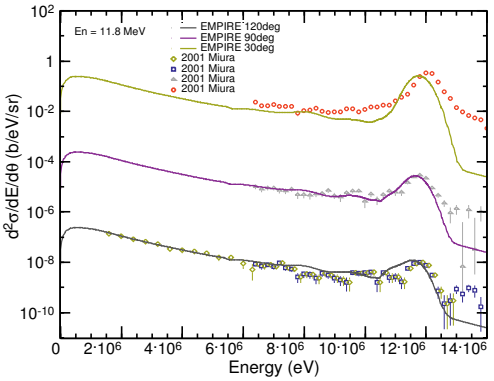

(d) Double-differential neutron emission spectra

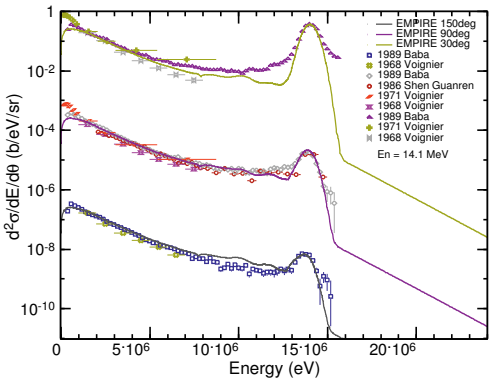

(e) Double-differential neutron emission spectra

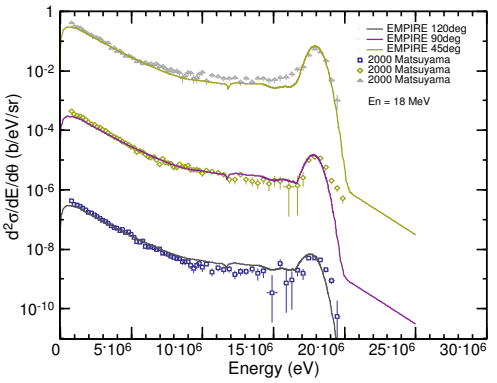

(f) Double-differential neutron emission spectra

Figure 9. EMPIRE calculated double-differential cross sections at selected angles and incident neutron energies. The experimental data were taken from the EXFOR database [8].

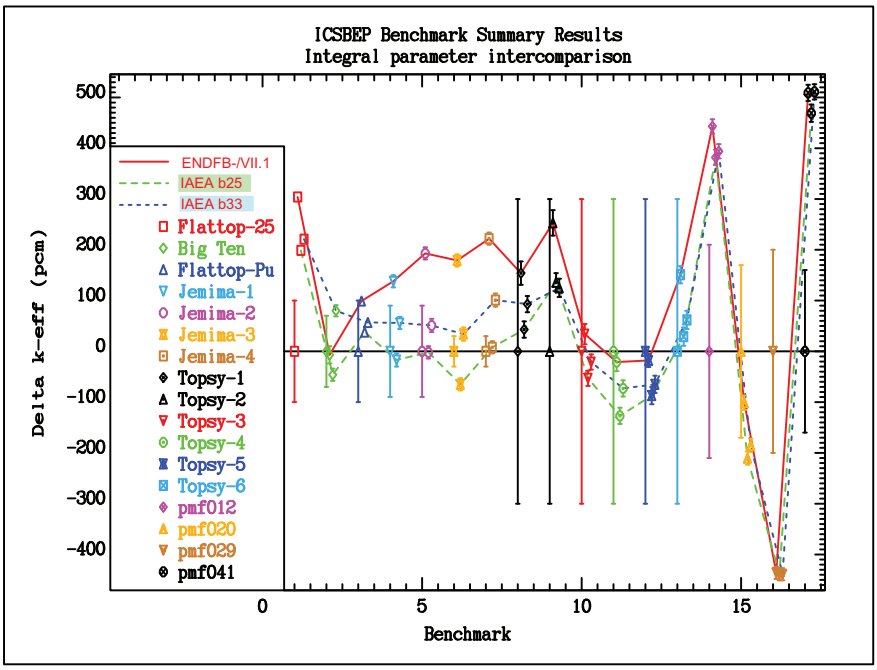

Figure 10. k_{eff} calculations for selected ICSBEP criticality benchmarks [18] sensitive to inelastic neutron scattering on ^{238}U. The calculation symbols are slightly shifted for clarity.

are performed at the level of model parameters and not at the cross-section level. This method guarantees the physical consistency of evaluated results in all iterations, which is not the case in typical adjustment methods.

- The procedure was reiterated and the results were improved: iteration *IAEA ib25* was reported in ref. [17], the current version is *IAEA ib33*. Unfortunately, it is a time consuming process as it involves scientists from different laboratories.

The results are very encouraging, we intend to continue this iterative procedure until they can be considered satisfactory. At that point, the EMPIRE-Monte Carlo-GANDR system will be used to produce the final evaluation including covariances.

3 Integral experiments

Benchmark experiments are measurements of integral parameters that can be accurately modelled by computation with very few assumptions and approximations. Typical compilations of this kind are contained in the Handbook of International Criticality Safety Benchmark Experiments [18]. A common practice in the past was to complete an evaluation, and then undertake the benchmarking exercises. This approach has a disadvantage that the feedback to the evaluators is very slow, and therefore an increased tendency has arisen to make benchmarking an integral part of the evaluation process (e.g. see Ref. [38]). Discrepancies between measurements and calculations can guide the evaluator where he/she has the flexibility to adjust certain model parameters that impact on calculated cross sections where no data exist, or discriminate between discrepant measurements of quantities that are being

evaluated. An example of improvements in the criticality benchmarks of evaluated nuclear data of ^{238}U (labelled *IAEA ib25* and *IAEA ib33*) compared with the data in the ENDF/B-VII.1 library [6] is shown in Fig.10. Differences are shown between the calculated and reference experimental values for selected criticality benchmarks that are very sensitive to the elastic and inelastic scattering data of ^{238}U. Improvements achieved in both *IAEA b25* and *IAEA b33* evaluations are particularly impressive for the JEMIMA benchmarks.

4 Conclusions

Reaction modelling advances have been applied to describe neutron induced reactions on the ^{238}U nucleus. A new dispersive optical model that couples almost all excited collective levels below 1 MeV of excitation energy has been very important to achieve a simultaneous description of elastic and inelastic neutron scattering cross sections and angular distributions in the whole energy range of interest. Interference between the direct and compound reactions predicted by Moldauer is shown to increase the calculated inelastic cross sections [34]; the cross-section increase is significant in the energy range from 100 to 500 keV. A better modelling of the elastic and inelastic scattering angular also implies the inclusion of the anisotropic (but symmetric relative to 90 degrees) compound-nucleus contribution at low energies, achieving an excellent description of the microscopic neutron scattering angular distributions from 50 keV up to around 3 MeV. Integral criticality benchmarks from the ICBESP Handbook (e.g. JEMIMA, FLATTOP-25, FLATTOP-Pu and BIGTEN assemblies) are used to assess the impact of advanced modelling on the elastic and inelastic cross sections. Performance of the current trial *IAEA ib33* evaluation on the selected benchmarks is shown to be better than the ENDF/B-VII.1 evaluation, and slightly better than the trial *IAEA ib25* evaluation [17]. Additional research is warranted.

Acknowledgments

The impact of quasi-differential data measured at RPI by Yaron Danon and collaborators on this evaluation can not be understated. The authors are grateful for our discussions. We also would like to thank all experimentalists who have contributed to the measured data used in our evaluation. Due to the comprehensive nature of the evaluation and space restrictions we could not list their original work and referred generically to the EXFOR database [8]. However, we recommend all readers to check data and refer to the original authors as listed in the figures for each calculated quantity. This evaluation would not have been possible without the hard work and endless efforts of a large number of individuals and institutions that produce the high quality experimental data shown in our figures.

References

[1] Uncertainty and target accuracy assessment for innovative systems using recent covariance data evaluations, Final report of the *NEA/WPEC-26*, Coordinator M. Salvatores, WPEC, (Nuclear Energy Agency, OECD 2008, Paris, France).

[2] A.J. Plompen, T. Kawano, R. Capote (Eds), Technical Meeting on Inelastic Scattering and Capture Cross-section Data of Major Actinides in the Fast Neutron Region, report **IAEA(NDS)-0597**, (International Atomic Energy Agency, Vienna, Austria, 2011).

[3] *Chinese Evaluated Nuclear Data Library CENDL-3.1*, China Nuclear Data Center, CD-ROM released on 24 December 2009.

[4] A. Koning *et al.*, The JEFF-3.1 Nuclear Data Library, *JEFF Report* **21** (NEA No. 6190, OECD 2006, Paris, France).

[5] K. Shibata *et al.*, JENDL-4.0: A New Library for Nuclear Science and Engineering, *J. Nucl. Sci. Technol.* **48**, 1 (2011).

[6] M.B. Chadwick *et al.*, *Nucl. Data Sheets* **112**, 2887 (2012).

[7] *ROSFOND-2010: Updated Russian library of evaluated neutron data*, IPPE, Obninsk, Russian Federation, 2010. Available online at *http://www.ippe.ru/podr/abbn/libr/rosfond.php*.

[8] *EXchange FORmat database (EXFOR)* is maintained by the Network of Nuclear Reaction Data Centers (see *http://www-nds.iaea.org/nrdc/*); data available online (e.g. at *http://www-nds.iaea.org/exfor/*).

[9] D.W.S. Chan, J.J. Egan, A. Mittler, and E. Sheldon, *Phys. Rev.* **C26**, 841–860 (1982).

[10] D.W.S. Chan and E. Sheldon, *Phys. Rev.* **C26**, 861–888 (1982).

[11] E. Sheldon *et al.*, *J.Phys.G: Nucl.Phys.* **12**, 443 (1986).

[12] T. Kawano, N. Fujikawa, and Y. Kanda. Evaluation of 238U inelastic scattering cross section. Tech. report JAERI-M-94-019,INDC(JPN)-169 (Japan Atomic Energy Research Institute, Ibaraki-ken, Japan, 1994).

[13] V. Maslov *et al.*. Neutron scattering on 238U and 232Th. In K. Shibata, editor, *International Conference on Nuclear Data for Science and Technology, October 7–12, Tsukuba, 2001*, Vol.1 (Atomic Energy Society of Japan, Japan, 2001), page 148.

[14] V.M. Maslov, Yu.V. Porodzinskij, N.A. Tetereva, M. Baba, and A. Hasegawa. *Nucl.Phys.***A764**, 212–245 (2006).

[15] M.J. Lopez Jimenez, B. Morillon, and P. Romain. *Ann. Nucl. Energy* **32**, 195–213 (2005).

[16] S. Badikov *et al.,* IAEA Scientific and Technical report **STI/PUB/1291** (IAEA, Vienna, 2008); A. D. Carlson *et al.*, *Nucl. Data Sheets* **110**, 3215 (2009).

[17] R. Capote, A. Trkov, M. Sin, M.W. Herman, A. Daskalakis, and Y. Danon *Nucl. Data Sheets* **115**, 26–31 (2014).

[18] *ICSBEP 2006*, International Handbook of Evaluated Criticality Safety Benchmark Experiments, Technical Report *NEA/NSC/DOC(95)03*, NEA Nuclear Science Committee, Nuclear Energy Agency (OECD 2006, Paris, France).

[19] M. Herman *et al.*, *Nucl. Data Sheets* **108**, 2655 (2007).

[20] M. Herman *et al.*, EMPIRE-3.2 Malta – Modular system for nuclear reaction calculations and nuclear data evaluation, report **INDC(NDS)-0603, BNL-101378-2013** (International Atomic Energy Agency, Vienna, Austria, August 2013).

[21] R. Capote *et al.*, *Nucl. Data Sheets* **110**, 3107 (2009) (see *http://www-nds.iaea.org/RIPL-3/*).

[22] E.Sh. Soukhovitskiĭ, R. Capote, J.M. Quesada and S. Chiba, *Phys. Rev.* **C72**, 024604 (2005).

[23] J.M. Quesada, R. Capote, A. Molina, M. Lozano, and J. Raynal. *Phys. Rev.***C67**, 067601 (2003).

[24] J.M. Quesada, E.Sh. Soukhovitskiĭ, R. Capote, S. Chiba, *Nucl. Data Sheets* **115**, xxx (2014), in press.

[25] J.M. Quesada, E.Sh. Soukhovitskiĭ, R. Capote and S. Chiba, EPJ Web of Conf. **42** (2013) 02005.

[26] E.Sh. Soukhovitskiĭ, S. Chiba, O. Iwamoto, K. Shibata, T. Fukahori, and G.B. Morogovskiĭ. *Programs OPTMAN and SHEMMAN Version 8*. Tech. report **JAERI-Data/Code 2005-002** (Japan Atomic Energy Research Institute, Ibaraki-ken, Japan, 2005).

[27] E.Sh. Soukhovitskiĭ, S. Chiba, R. Capote, J.M. Quesada *et al.*, Tech. report **JAERI-Data/Code 2008-025** (Japan Atomic Energy Research Institute, Ibaraki-ken, Japan, 2008).

[28] R. Capote, S. Chiba, E.Sh. Soukhovitskiĭ, J. M. Quesada, and E. Bauge. *J. of Nucl. Sc. Tech.* **45**, 333–340 (2008).
[29] W. Hauser, H. Feshbach, *Phys. Rev.* **87**, 366 (1952).
[30] H.M. Hofmann, J. Richert, J.W. Tepel, H.A. Weidenmüller, *Ann. Phys.* **90**, 403 (1975).
[31] M. Sin, R. Capote, A. Ventura, M. Herman, P. Obložinský, *Phys. Rev.* **C74**, 014608 (2006).
[32] M. Sin, R. Capote, *Phys. Rev.* **C77**, 054601 (2008).
[33] R. Capote, D.L. Smith, A. Trkov, *EPJ Web of Conferences* **8**, 04001 (2010).
[34] P.A. Moldauer, *Phys. Rev.* **C12**, 744 (1975).
[35] C.A. Engelbrecht, H.A. Weidenmüller, *Phys. Rev.* **C8**, 859 (1973).
[36] J. Raynal, Optical model and coupled-channel calculations in nuclear physics, p.281, *Computing as a language of physics, ICTP International Seminar Course, Trieste, Italy, 1971* (International Atomic Energy Agency, Vienna, Austria, 1972).
[37] Y. Danon *et al.*, presentation at Int. Workshop on Elastic and Inelastic Scattering, WINS-2012, Boston, 17-19 September 2012.
[38] A. Trkov *et al.*, *Nucl. Data Sheets* **112**, 3098 (2011).